Regular Article - Experimental Physics

Measurement of Υ production in pp collisions at $\sqrt{s} = 7$ TeV

The LHCb Collaboration[⋆]

CERN, 1211 Geneva 23, Switzerland

Abstract The production of $\Upsilon(1S)$, $\Upsilon(2S)$ and $\Upsilon(3S)$ mesons in proton-proton collisions at the centre-of-mass energy of $\sqrt{s} = 7$ TeV is studied with the LHCb detector. The analysis is based on a data sample of 25 pb^{-1} collected at the Large Hadron Collider. The Υ mesons are reconstructed in the decay mode $\Upsilon \to \mu^+\mu^-$ and the signal yields are extracted from a fit to the $\mu^+\mu^-$ invariant mass distributions. The differential production cross-sections times dimuon branching fractions are measured as a function of the Υ transverse momentum p_T and rapidity y, over the range $p_T < 15$ GeV/c and $2.0 < y < 4.5$. The cross-sections times branching fractions, integrated over these kinematic ranges, are measured to be

$$\sigma\big(pp \to \Upsilon(1S)X\big) \times \mathcal{B}\big(\Upsilon(1S) \to \mu^+\mu^-\big)$$
$$= 2.29 \pm 0.01 \pm 0.10^{+0.19}_{-0.37} \text{ nb},$$
$$\sigma\big(pp \to \Upsilon(2S)X\big) \times \mathcal{B}\big(\Upsilon(2S) \to \mu^+\mu^-\big)$$
$$= 0.562 \pm 0.007 \pm 0.023^{+0.048}_{-0.092} \text{ nb},$$
$$\sigma\big(pp \to \Upsilon(3S)X\big) \times \mathcal{B}\big(\Upsilon(3S) \to \mu^+\mu^-\big)$$
$$= 0.283 \pm 0.005 \pm 0.012^{+0.025}_{-0.048} \text{ nb},$$

where the first uncertainty is statistical, the second systematic and the third is due to the unknown polarisation of the three Υ states.

1 Introduction

The measurement of heavy quark production in hadron collisions probes the dynamics of the colliding partons. The study of heavy quark–antiquark resonances, such as the $b\bar{b}$ bound states $\Upsilon(1S)$, $\Upsilon(2S)$ and $\Upsilon(3S)$ (indicated generically as Υ in the following) is of interest as these mesons have large production cross-sections and can be produced in different spin configurations. In addition, the

thorough understanding of these states is the first step towards the study of recently discovered new states in the $b\bar{b}$ system [1–4]. Although Υ production was studied by several experiments in the past, the underlying production mechanism is still not well understood. Several models exist but fail to reproduce both the cross-section and the polarisation measurements at the Tevatron [5–7]. Among these are the Colour Singlet Model (CSM) [8–10], recently improved by adding higher order contributions (NLO CSM), the standard truncation of the nonrelativistic QCD expansion (NRQCD) [11], which includes contributions from the Colour Octet Mechanism [12, 13], and the Colour Evaporation Model (CEM) [14]. Although the disagreement of the theory with the data is less pronounced for bottomonium than for charmonium, the measurement of Υ production is important as the theoretical calculations are more robust due to the heavier bottom quark.

There are two major sources of Υ production in pp collisions: direct production and feed-down from the decay of heavier prompt bottomonium states, like χ_b, or higher-mass Υ states. This study presents measurements of the individual inclusive production cross-sections of the three Υ mesons decaying into a pair of muons. The measurements are performed in 7 TeV centre-of-mass pp collisions as a function of the Υ transverse momentum ($p_T < 15$ GeV/c) and rapidity ($2 < y < 4.5$), in 15 bins of p_T and five bins of y. This analysis is complementary to those recently presented by the ATLAS collaboration, who measured the $\Upsilon(1S)$ cross section for $|y| < 2.4$ [15], and the CMS collaboration, who measured the $\Upsilon(1S)$, $\Upsilon(2S)$ and $\Upsilon(3S)$ cross sections in the rapidity region $|y| < 2.0$ [16].

2 The LHCb detector and data

The results presented here are based on a dataset of 25.0 ± 0.9 pb^{-1} collected at the Large Hadron Collider (LHC) in 2010 with the LHCb detector at a centre-of-mass energy of 7 TeV.

⋆ e-mail: giulia.manca@cern.ch

The LHCb detector [17] is a single-arm forward spectrometer covering the pseudo-rapidity range $2 < \eta < 5$, designed for the study of particles containing b or c quarks. The detector includes a high precision tracking system consisting of a silicon-strip vertex detector surrounding the pp interaction region, a large-area silicon-strip detector located upstream of a dipole magnet with a bending power of about 4 Tm, and three stations of silicon-strip detectors and straw drift-tubes placed downstream. The combined tracking system has a momentum resolution $\Delta p/p$ that varies from 0.4 % at 5 GeV/c to 0.6 % at 100 GeV/c, and an impact parameter resolution of 20 μm for tracks with high transverse momentum. Charged hadrons are identified using two ring-imaging Cherenkov detectors. Photon, electron and hadron candidates are identified by a calorimeter system consisting of scintillating-pad and pre-shower detectors, an electromagnetic calorimeter and a hadronic calorimeter. Muons are identified by a muon system composed of alternating layers of iron and multiwire proportional chambers. The trigger consists of a hardware stage, based on information from the calorimeter and muon systems, followed by a software stage which applies a full event reconstruction. This analysis uses events triggered by one or two muons. At the hardware level one or two muon candidates are required with p_T larger than 1.4 GeV/c for one muon, and 0.56 and 0.48 GeV/c for two muons. At the software level, the combined dimuon mass is required to be greater than 2.9 GeV/c^2, and both the tracks and the vertex have to be of good quality. To avoid the possibility that a few events with a high occupancy dominate the trigger processing time, a set of global event selection requirements based on hit multiplicities is applied.

The Monte Carlo samples used are based on the PYTHIA 6.4 generator [18], with a choice of parameters specifically configured for LHCb [19]. The EVTGEN package [20] describes the decay of the Υ resonances, and the GEANT4 package [21] simulates the detector response. The prompt bottomonium production processes activated in PYTHIA are those from the leading-order colour-singlet and colour-octet mechanisms for the $\Upsilon(1S)$, and colour-singlet only for the $\Upsilon(2S)$ and the $\Upsilon(3S)$. QED radiative corrections to the decay $\Upsilon \rightarrow \mu^+\mu^-$ are generated with the PHOTOS package [22].

3 Cross-section determination

The double differential cross-section for the inclusive Υ production of the three different states is computed as

$$\frac{d^2\sigma^{iS}}{dp_T dy} \times \mathcal{B}^{iS} = \frac{N^{iS}}{\mathcal{L} \times \varepsilon^{iS} \times \Delta y \times \Delta p_T}, \quad i = 1, 2, 3; \quad (1)$$

where σ^{iS} is the inclusive cross section $\sigma(pp \rightarrow \Upsilon(iS)X)$, $\mathcal{B}^{iS}$ is the dimuon branching fraction $\mathcal{B}(\Upsilon(iS) \rightarrow \mu^+\mu^-)$,

N^{iS} is the number of observed $\Upsilon(iS) \rightarrow \mu^+\mu^-$ decays in a given bin of p_T and y, ε^{iS} is the $\Upsilon(iS) \rightarrow \mu^+\mu^-$ total detection efficiency including acceptance effects, $\mathcal{L}$ is the integrated luminosity and $\Delta y = 0.5$ and $\Delta p_T = 1$ GeV/c are the rapidity and p_T bin sizes, respectively. In order to estimate N^{iS}, a fit to the reconstructed invariant mass distribution is performed in each of the 15 $p_T \times 5$ y bins. Υ candidates are formed from pairs of oppositely charged muon tracks which traverse the full spectrometer and satisfy the trigger requirements. Each track must have $p_T > 1$ GeV/c, be identified as a muon and have a good quality of the track fit. The two muons are required to originate from a common vertex with a good χ^2 probability. The three Υ signal yields are determined from a fit to the reconstructed invariant mass m of the selected Υ candidates in the interval 8.9–10.9 GeV/c^2. The mass distribution is described by a sum of three Crystal Ball functions [23] for the $\Upsilon(1S)$, $\Upsilon(2S)$ and $\Upsilon(3S)$ signals and an exponential function for the combinatorial background. The Crystal Ball function is defined as

$$f_{CB} = \begin{cases} \frac{(\frac{n}{|a|})^n e^{-\frac{1}{2}a^2}}{(\frac{n}{|a|} - |a| - \frac{m-M}{\sigma})^n} & \text{if } \frac{m-M}{\sigma} < -|a| \\ \exp\left(-\frac{1}{2}\left(\frac{m-M}{\sigma}\right)^2\right) & \text{otherwise,} \end{cases} \quad (2)$$

with $f_{CB} = f_{CB}(m; M, \sigma, a, n)$, where M and σ are the mean and width of the gaussian. The parameters a and n describing the radiative tail of the Υ mass distribution are fixed to describe a tail dominated by QED photon emission, as confirmed by simulation. The distribution in Fig. 1 shows the results of the fit performed in the full range of p_T and y. The signal yields obtained from the fit are $\Upsilon(1S) = 26410 \pm 212$, $\Upsilon(2S) = 6726 \pm 142$ and $\Upsilon(3S) = 3260 \pm 112$ events. The mass resolution of the $\Upsilon(1S)$ peak is $\sigma = 53.9 \pm 0.5$ MeV/c^2. The resolutions of the $\Upsilon(2S)$
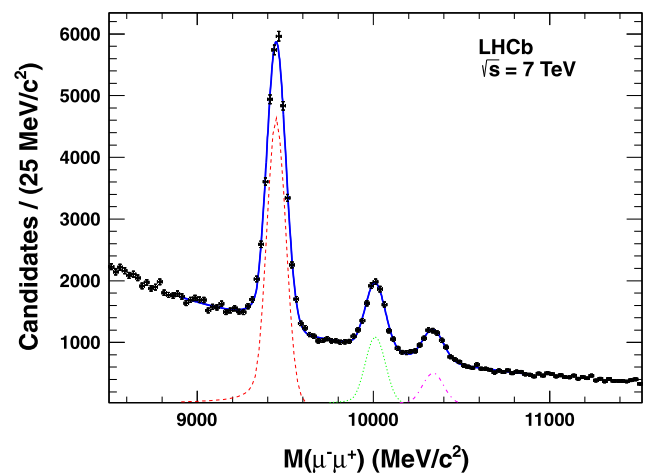
Fig. 1 Invariant mass distribution of the selected $\Upsilon \rightarrow \mu^+\mu^-$ candidates in the range $p_T < 15$ GeV/c and $2.0 < y < 4.5$. The three peaks correspond to the $\Upsilon(1S)$, $\Upsilon(2S)$ and $\Upsilon(3S)$ signals (*from left to right*). The superimposed curves are the result of the fit as described in the text
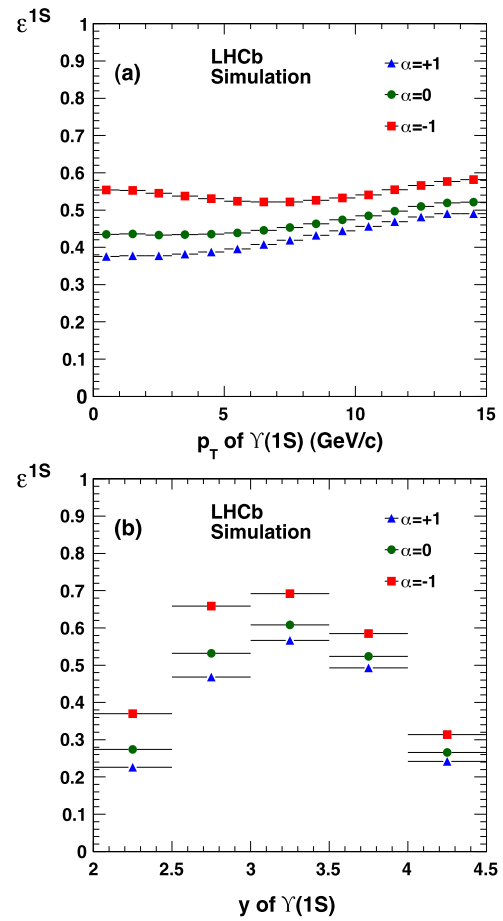
and $\Upsilon(3S)$ peaks are fixed to the resolution of the $\Upsilon(1S)$, scaled by the ratio of the masses, as expected from resolution effects. The masses are allowed to vary in the fit and are measured to be $M(\Upsilon(1S)) = 9448.3 \pm 0.5$ MeV/c^2, $M(\Upsilon(2S)) = 10\,010.4 \pm 1.4$ MeV/c^2 and $M(\Upsilon(3S)) = 10\,338.7 \pm 2.6$ MeV/c^2, where the quoted uncertainties are statistical only. The fit is repeated independently for each of the bins in p_T and y. When fitting the individual bins, due to the reduced dataset, the masses and widths of the three Υ states in the fit are fixed to the values obtained when fitting the full range. Bins with fewer than 36 entries are excluded from the analysis. The total efficiency ε entering the cross-section expression of (1) is the product of the geometric acceptance, the reconstruction and selection efficiency and the trigger efficiency. All efficiency terms have been evaluated using Monte Carlo simulations in each (p_T, y) bin separately, with the exception of that related to the global event selection which has been determined from data. In the simulation the Υ meson is produced in an unpolarised state. The absolute luminosity scale was measured at specific periods during the 2010 data taking using both van der Meer scans and a beam-gas imaging method [24, 25]. The uncertainty on the integrated luminosity for the analysed sample due to this method is estimated to be 3.5 % [25]. The knowledge of the absolute luminosity scale is used to calibrate the number of tracks in the vertex detector, which is found to be stable throughout the data-taking period and can therefore be used to monitor the instantaneous luminosity of the entire data sample. The integrated luminosity of the data sample used in this analysis is determined to be 25.0 pb^{-1}.

Fig. 2 Total efficiency ε of the $\Upsilon(1S)$ as a function of (**a**) the $\Upsilon(1S)$ transverse momentum and (**b**) rapidity, estimated using the Monte Carlo simulation, for three different $\Upsilon(1S)$ polarisation scenarios, indicated by the parameter α described in the text

4 Systematic uncertainties

Extensive studies on dimuon decays [15, 16, 26] have shown that the total efficiency depends strongly on the initial polarisation state of the vector meson. In this analysis, the influence of the unknown polarisation is studied in the helicity frame [27] using Monte Carlo simulation. The angular distribution of the muons from the Υ, ignoring the azimuthal part, is

$$\frac{dN}{d\cos\theta} = \frac{1 + \alpha \cos^2\theta}{2 + 2\alpha/3}, \tag{3}$$

where θ is the angle between the direction of the μ^+ momentum in the Υ centre-of-mass frame and the direction of the Υ momentum in the colliding proton centre-of-mass frame. The values $\alpha = +1, -1, 0$ correspond to fully transverse, fully longitudinal, and no polarisation respectively. Figure 2 shows the $\Upsilon(1S)$ total efficiency for these three scenarios, and indicates that the polarisation signifi-

cantly affects the efficiencies and that the effect depends on p_T and y. A similar behaviour is observed for the $\Upsilon(2S)$ and $\Upsilon(3S)$ efficiencies. Following this observation, in each (p_T, y) bin the maximal difference between the polarised scenarios ($\alpha = \pm 1$) and the unpolarised scenario ($\alpha = 0$) is taken as a systematic uncertainty on the efficiency. This results in an uncertainty of up to 17 % on the integrated cross-sections and of up to 40 % in the individual bins. Several other sources of possible systematic effects were studied. They are summarised in Table 1.

The trigger efficiency is determined on data using an unbiased sample of events that would trigger if the Υ candidate were removed. The efficiency obtained with this method is compared with the efficiency determined in the simulation. The difference of 3.0 % is assigned as a systematic uncertainty.

The uncertainty on the muon track reconstruction efficiency has been estimated using a data driven tag-and-probe approach based on partially reconstructed $J/\psi \to \mu^+\mu^-$ decays [28], and found to be 2.4 % per muon pair. Addi-

Table 1 Summary of the relative systematic uncertainties on the cross-section measurements. Ranges indicate variations depending on the (p_T, y) bin and the Υ state. All uncertainties are fully correlated among the bins

Source	Uncertainty (%)
Unknown Υ polarisation	0.3–41.0
Trigger	3.0
Track reconstruction	2.4
Track quality requirement	0.5
Vertexing requirement	1.0
Muon identification	1.1
Global event selection requirements	0.6
p_T binning effect	1.0
Fit function	1.1–2.1
Luminosity	3.5

tional uncertainties are assigned, which account for the different behaviour in data and simulation of the track and vertex quality requirements. The muon identification efficiency is measured using a tag-and-probe approach, which gives an uncertainty on the efficiency of 1.1 % [26].

The measurement of the global event selection efficiency is taken as an additional uncertainty associated with the trigger. An uncertainty of 1.0 % is considered to account for the difference in the p_T spectra in data and Monte Carlo simulation for the three Υ states, which might have an effect on the correct bin assignment ("binning effect").

The influence of the choice of the fit function describing the shape of the invariant mass distribution includes two components. The uncertainty on the shape of the background distribution is estimated using a different fit model (1.0–1.5 %). The systematic associated with fixing the parameters of the Crystal Ball function is estimated by varying the central values within the parameters uncertainties, obtained when leaving them free to vary in the fit (0.5–1.4 %).

5 Results

The double differential cross-sections as a function of p_T and y are shown in Fig. 3 and Tables 2, 3, 4. The integrated cross-sections times branching fractions in the range $p_T < 15$ GeV/c and $2.0 < y < 4.5$ are measured to be

$$\sigma(pp \to \Upsilon(1S)X) \times \mathcal{B}^{1S}$$
$$= 2.29 \pm 0.01 \pm 0.10^{+0.19}_{-0.37} \text{ nb},$$

$$\sigma(pp \to \Upsilon(2S)X) \times \mathcal{B}^{2S}$$
$$= 0.562 \pm 0.007 \pm 0.023^{+0.048}_{-0.092} \text{ nb},$$
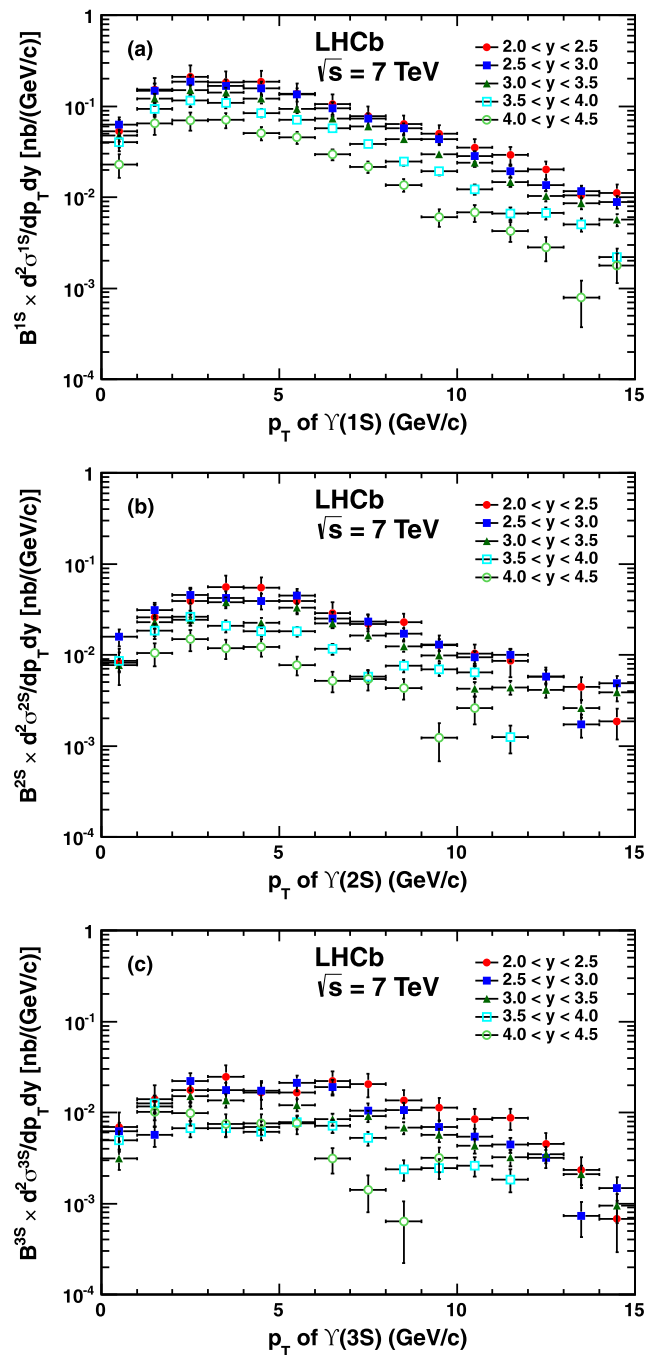
Fig. 3 Double differential $\Upsilon \to \mu^+\mu^-$ cross-sections times dimuon branching fractions as a function of p_T in bins of rapidity for (**a**) the $\Upsilon(1S)$, (**b**) the $\Upsilon(2S)$ and (**c**) the $\Upsilon(3S)$. The *error bars* correspond to the total uncertainty for each bin

$$\sigma(pp \to \Upsilon(3S)X) \times \mathcal{B}^{3S}$$
$$= 0.283 \pm 0.005 \pm 0.012^{+0.025}_{-0.048} \text{ nb},$$

where the first uncertainties are statistical, the second systematic and the third are due to the unknown polarisation of the three Υ states. The integrated $\Upsilon(1S)$ cross-section

Table 2 Double differential cross-section $\Upsilon(1S) \to \mu^+\mu^-$ as a function of rapidity and transverse momentum, in pb/(GeV/c). The first uncertainty is statistical, the second is systematic, and the third is due to the unknown polarisation of the $\Upsilon(1S)$

p_{T} (GeV/c)	$2.0 < y < 2.5$	$2.5 < y < 3.0$	$3.0 < y < 3.5$	$3.5 < y < 4.0$	$4.0 < y < 4.5$
0–1	$53.1 \pm 4.0 \pm 2.5^{+8.9}_{-17.3}$	$62.6 \pm 3.0 \pm 2.9^{+6.1}_{-11.5}$	$48.0 \pm 2.4 \pm 2.2^{+3.1}_{-5.8}$	$40.1 \pm 2.4 \pm 1.9^{+3.9}_{-7.0}$	$22.9 \pm 2.7 \pm 1.1^{+3.4}_{-5.9}$
1–2	$152.5 \pm 6.8 \pm 7.2^{+25.7}_{-50.4}$	$148.8 \pm 4.7 \pm 7.0^{+14.6}_{-27.5}$	$120.5 \pm 3.8 \pm 5.6^{+7.5}_{-14.0}$	$93.3 \pm 3.7 \pm 4.3^{+8.1}_{-14.8}$	$64.5 \pm 4.5 \pm 3.0^{+8.7}_{-15.0}$
2–3	$211.0 \pm 8.0 \pm 10.0^{+34.3}_{-67.2}$	$185.3 \pm 5.2 \pm 8.7^{+18.1}_{-34.4}$	$150.0 \pm 4.3 \pm 7.0^{+9.2}_{-17.4}$	$116.1 \pm 4.1 \pm 5.4^{+8.4}_{-15.5}$	$69.8 \pm 4.6 \pm 3.3^{+8.3}_{-14.6}$
3–4	$184.3 \pm 7.3 \pm 8.8^{+28.8}_{-56.3}$	$167.7 \pm 4.9 \pm 7.9^{+15.6}_{-29.3}$	$141.9 \pm 4.2 \pm 6.6^{+8.0}_{-15.0}$	$109.7 \pm 4.0 \pm 5.1^{+6.3}_{-11.9}$	$70.6 \pm 4.6 \pm 3.3^{+6.7}_{-12.2}$
4–5	$187.3 \pm 7.3 \pm 8.9^{+27.9}_{-54.8}$	$158.4 \pm 4.8 \pm 7.4^{+14.0}_{-26.4}$	$120.9 \pm 3.9 \pm 5.7^{+6.0}_{-11.3}$	$84.6 \pm 3.5 \pm 4.0^{+3.7}_{-7.0}$	$50.4 \pm 3.8 \pm 2.4^{+3.7}_{-7.0}$
5–6	$138.0 \pm 6.2 \pm 6.6^{+19.4}_{-38.3}$	$134.5 \pm 4.4 \pm 6.3^{+11.0}_{-20.8}$	$94.2 \pm 3.5 \pm 4.4^{+3.8}_{-7.3}$	$70.6 \pm 3.2 \pm 3.3^{+2.1}_{-4.0}$	$45.3 \pm 3.6 \pm 2.1^{+2.5}_{-4.9}$
6–7	$105.3 \pm 5.3 \pm 5.0^{+14.0}_{-27.6}$	$95.2 \pm 3.7 \pm 4.5^{+7.2}_{-13.7}$	$73.5 \pm 3.0 \pm 3.5^{+2.4}_{-4.6}$	$57.0 \pm 2.9 \pm 2.7^{+1.0}_{-1.9}$	$29.5 \pm 2.8 \pm 1.4^{+1.2}_{-2.5}$
7–8	$78.3 \pm 4.5 \pm 3.7^{+9.8}_{-19.4}$	$72.9 \pm 3.2 \pm 3.4^{+5.0}_{-9.6}$	$60.2 \pm 2.7 \pm 2.8^{+1.6}_{-3.0}$	$38.3 \pm 2.3 \pm 1.8^{+0.4}_{-0.8}$	$21.6 \pm 2.4 \pm 1.0^{+0.7}_{-1.5}$
8–9	$63.5 \pm 4.0 \pm 3.0^{+7.5}_{-14.8}$	$57.0 \pm 2.8 \pm 2.7^{+3.6}_{-6.8}$	$43.3 \pm 2.3 \pm 2.0^{+1.0}_{-1.9}$	$24.7 \pm 1.9 \pm 1.2^{+0.3}_{-0.6}$	$13.6 \pm 1.9 \pm 0.6^{+0.4}_{-0.8}$
9–10	$50.1 \pm 3.5 \pm 2.4^{+5.5}_{-10.8}$	$43.2 \pm 2.4 \pm 2.0^{+2.6}_{-5.0}$	$29.8 \pm 1.9 \pm 1.4^{+0.5}_{-1.0}$	$19.4 \pm 1.6 \pm 0.9^{+0.3}_{-0.6}$	$6.1 \pm 1.2 \pm 0.3^{+0.1}_{-0.3}$
10–11	$35.4 \pm 2.9 \pm 1.7^{+3.7}_{-7.3}$	$28.2 \pm 1.9 \pm 1.3^{+1.6}_{-3.0}$	$23.9 \pm 1.7 \pm 1.1^{+0.4}_{-0.8}$	$12.3 \pm 1.3 \pm 0.6^{+0.2}_{-0.5}$	$6.8 \pm 1.3 \pm 0.3^{+0.2}_{-0.4}$
11–12	$29.3 \pm 2.6 \pm 1.4^{+2.9}_{-5.8}$	$19.4 \pm 1.6 \pm 0.9^{+1.0}_{-1.9}$	$14.7 \pm 1.3 \pm 0.7^{+0.3}_{-0.6}$	$6.7 \pm 0.9 \pm 0.3^{+0.1}_{-0.2}$	$4.3 \pm 1.0 \pm 0.2^{+0.1}_{-0.3}$
12–13	$20.3 \pm 2.1 \pm 1.0^{+1.9}_{-3.7}$	$13.7 \pm 1.3 \pm 0.6^{+0.7}_{-1.3}$	$10.3 \pm 1.1 \pm 0.5^{+0.2}_{-0.3}$	$6.7 \pm 0.9 \pm 0.3^{+0.1}_{-0.2}$	$2.8 \pm 0.8 \pm 0.1^{+0.1}_{-0.2}$
13–14	$10.4 \pm 1.5 \pm 0.5^{+0.9}_{-1.9}$	$11.6 \pm 1.2 \pm 0.5^{+0.6}_{-1.1}$	$8.6 \pm 1.0 \pm 0.4^{+0.1}_{-0.2}$	$5.0 \pm 0.8 \pm 0.2^{+0.1}_{-0.1}$	$0.8 \pm 0.4 \pm 0.0^{+0.0}_{-0.1}$
14–15	$11.2 \pm 1.5 \pm 0.5^{+1.0}_{-2.0}$	$8.9 \pm 1.0 \pm 0.4^{+0.4}_{-0.8}$	$5.7 \pm 0.8 \pm 0.3^{+0.1}_{-0.2}$	$2.2 \pm 0.5 \pm 0.1^{+0.0}_{-0.1}$	$1.8 \pm 0.6 \pm 0.1^{+0.1}_{-0.1}$

Table 3 Double differential cross-section $\Upsilon(2S) \to \mu^+\mu^-$ as a function of rapidity and transverse momentum, in pb/(GeV/c). The first uncertainty is statistical, the second is systematic, and the third is due to the unknown polarisation of the $\Upsilon(2S)$. Regions where the number of events was not sufficient to perform a measurement are indicated with a *dash*

p_{T} (GeV/c)	$2.0 < y < 2.5$	$2.5 < y < 3.0$	$3.0 < y < 3.5$	$3.5 < y < 4.0$	$4.0 < y < 4.5$
0–1	$8.2 \pm 1.7 \pm 0.4^{+1.5}_{-3.1}$	$15.8 \pm 1.6 \pm 0.7^{+1.5}_{-2.8}$	$7.8 \pm 1.0 \pm 0.4^{+0.4}_{-0.8}$	$8.6 \pm 1.2 \pm 0.4^{+0.8}_{-1.5}$	–
1–2	$25.8 \pm 2.9 \pm 1.2^{+4.6}_{-9.2}$	$31.2 \pm 2.2 \pm 1.5^{+3.1}_{-5.6}$	$23.0 \pm 1.7 \pm 1.1^{+1.6}_{-2.9}$	$18.3 \pm 1.6 \pm 0.9^{+1.6}_{-2.8}$	$10.4 \pm 1.8 \pm 0.5^{+1.4}_{-2.3}$
2–3	$39.3 \pm 3.6 \pm 1.9^{+6.4}_{-12.9}$	$45.7 \pm 2.6 \pm 2.1^{+4.5}_{-8.2}$	$24.4 \pm 1.8 \pm 1.1^{+1.5}_{-2.9}$	$26.3 \pm 2.0 \pm 1.2^{+1.9}_{-3.4}$	$14.9 \pm 2.2 \pm 0.7^{+1.8}_{-3.2}$
3–4	$55.8 \pm 4.2 \pm 2.6^{+8.9}_{-17.4}$	$42.1 \pm 2.5 \pm 2.0^{+3.8}_{-7.3}$	$37.8 \pm 2.2 \pm 1.8^{+2.2}_{-4.3}$	$20.8 \pm 1.8 \pm 1.0^{+1.3}_{-2.4}$	$11.9 \pm 1.9 \pm 0.6^{+1.2}_{-2.1}$
4–5	$54.5 \pm 4.1 \pm 2.6^{+8.2}_{-15.9}$	$39.2 \pm 2.4 \pm 1.8^{+3.6}_{-6.7}$	$22.6 \pm 1.7 \pm 1.1^{+1.1}_{-2.0}$	$18.3 \pm 1.6 \pm 0.9^{+0.8}_{-1.6}$	$12.2 \pm 1.9 \pm 0.6^{+1.0}_{-1.8}$
5–6	$39.1 \pm 3.4 \pm 1.9^{+5.4}_{-10.3}$	$44.8 \pm 2.6 \pm 2.1^{+3.9}_{-7.6}$	$32.8 \pm 2.1 \pm 1.5^{+1.5}_{-2.8}$	$18.1 \pm 1.6 \pm 0.8^{+0.6}_{-1.2}$	$7.8 \pm 1.5 \pm 0.4^{+0.4}_{-0.9}$
6–7	$28.8 \pm 2.9 \pm 1.4^{+4.1}_{-8.3}$	$25.1 \pm 1.9 \pm 1.2^{+2.0}_{-3.9}$	$22.3 \pm 1.7 \pm 1.0^{+0.7}_{-1.4}$	$11.6 \pm 1.3 \pm 0.5^{+0.3}_{-0.5}$	$5.2 \pm 1.2 \pm 0.2^{+0.2}_{-0.5}$
7–8	$21.9 \pm 2.4 \pm 1.0^{+2.7}_{-5.4}$	$23.4 \pm 1.9 \pm 1.1^{+1.8}_{-3.5}$	$16.3 \pm 1.4 \pm 0.8^{+0.4}_{-0.9}$	$5.8 \pm 0.9 \pm 0.3^{+0.1}_{-0.1}$	$5.4 \pm 1.2 \pm 0.3^{+0.2}_{-0.4}$
8–9	$22.9 \pm 2.4 \pm 1.1^{+2.6}_{-4.8}$	$17.1 \pm 1.5 \pm 0.8^{+1.0}_{-2.0}$	$12.4 \pm 1.2 \pm 0.6^{+0.3}_{-0.6}$	$7.6 \pm 1.0 \pm 0.4^{+0.1}_{-0.2}$	$4.3 \pm 1.0 \pm 0.2^{+0.1}_{-0.3}$
9–10	$12.8 \pm 1.8 \pm 0.6^{+1.5}_{-2.9}$	$12.9 \pm 1.3 \pm 0.6^{+0.6}_{-1.2}$	$9.8 \pm 1.1 \pm 0.5^{+0.2}_{-0.5}$	$7.0 \pm 1.0 \pm 0.3^{+0.1}_{-0.2}$	$1.2 \pm 0.5 \pm 0.1^{+0.0}_{-0.1}$
10–11	$10.3 \pm 1.6 \pm 0.5^{+1.1}_{-2.1}$	$9.5 \pm 1.1 \pm 0.4^{+0.5}_{-0.9}$	$4.3 \pm 0.7 \pm 0.2^{+0.1}_{-0.2}$	$6.4 \pm 0.9 \pm 0.3^{+0.1}_{-0.2}$	$2.6 \pm 0.8 \pm 0.1^{+0.1}_{-0.2}$
11–12	$8.6 \pm 1.5 \pm 0.4^{+1.2}_{-2.4}$	$10.0 \pm 1.1 \pm 0.5^{+0.5}_{-0.9}$	$4.4 \pm 0.7 \pm 0.2^{+0.0}_{-0.1}$	$1.2 \pm 0.4 \pm 0.1^{+0.0}_{-0.0}$	–
12–13	$5.8 \pm 1.2 \pm 0.3^{+0.5}_{-0.9}$	$5.8 \pm 0.9 \pm 0.3^{+0.3}_{-0.5}$	$4.1 \pm 0.7 \pm 0.2^{+0.0}_{-0.1}$	–	–
13–14	$4.4 \pm 1.0 \pm 0.2^{+0.4}_{-0.7}$	$1.7 \pm 0.5 \pm 0.1^{+0.1}_{-0.1}$	$2.6 \pm 0.5 \pm 0.1^{+0.0}_{-0.1}$	–	–
14–15	$1.9 \pm 0.6 \pm 0.1^{+0.2}_{-0.3}$	$4.9 \pm 0.8 \pm 0.2^{+0.3}_{-0.5}$	$3.9 \pm 0.7 \pm 0.2^{+0.1}_{-0.3}$	–	–

Table 4 Double differential cross-section $\Upsilon(3S) \to \mu^+\mu^-$ as a function of rapidity and transverse momentum, in pb/(GeV/c). The first uncertainty is statistical, the second is systematic, and the third is due to the unknown polarisation of the $\Upsilon(3S)$. Regions where the number of events was not sufficient to perform a measurement are indicated with a *dash*

p_T (GeV/c)	$2.0 < y < 2.5$	$2.5 < y < 3.0$	$3.0 < y < 3.5$	$3.5 < y < 4.0$	$4.0 < y < 4.5$
0–1	$7.0 \pm 1.5 \pm 0.3^{+1.3}_{-2.6}$	$6.3 \pm 1.0 \pm 0.3^{+0.6}_{-1.0}$	$3.1 \pm 0.6 \pm 0.1^{+0.2}_{-0.4}$	$5.0 \pm 0.9 \pm 0.2^{+0.5}_{-0.9}$	–
1–2	$14.1 \pm 2.2 \pm 0.7^{+2.6}_{-5.3}$	$5.6 \pm 0.9 \pm 0.3^{+0.6}_{-1.1}$	$11.6 \pm 1.2 \pm 0.6^{+0.7}_{-1.3}$	$12.7 \pm 1.4 \pm 0.6^{+1.2}_{-2.1}$	$10.2 \pm 1.9 \pm 0.5^{+1.4}_{-2.6}$
2–3	$17.6 \pm 2.3 \pm 0.9^{+2.7}_{-5.3}$	$22.3 \pm 1.8 \pm 1.1^{+2.1}_{-4.1}$	$15.2 \pm 1.4 \pm 0.7^{+0.8}_{-1.6}$	$6.7 \pm 1.0 \pm 0.3^{+0.5}_{-0.9}$	$9.9 \pm 1.7 \pm 0.5^{+1.2}_{-2.1}$
3–4	$24.9 \pm 2.7 \pm 1.2^{+4.0}_{-7.7}$	$17.6 \pm 1.6 \pm 0.8^{+1.6}_{-3.1}$	$13.5 \pm 1.3 \pm 0.6^{+0.8}_{-1.6}$	$6.8 \pm 1.0 \pm 0.3^{+0.4}_{-0.8}$	$7.5 \pm 1.5 \pm 0.4^{+0.7}_{-1.3}$
4–5	$16.7 \pm 2.2 \pm 0.8^{+2.6}_{-5.1}$	$17.5 \pm 1.6 \pm 0.8^{+1.6}_{-3.0}$	$6.9 \pm 0.9 \pm 0.3^{+0.3}_{-0.6}$	$6.1 \pm 0.9 \pm 0.3^{+0.3}_{-0.5}$	$7.6 \pm 1.5 \pm 0.4^{+0.6}_{-1.2}$
5–6	$16.6 \pm 2.1 \pm 0.8^{+2.4}_{-4.6}$	$21.3 \pm 1.8 \pm 1.0^{+1.8}_{-3.5}$	$12.1 \pm 1.2 \pm 0.6^{+0.6}_{-1.1}$	$7.8 \pm 1.1 \pm 0.4^{+0.3}_{-0.5}$	$7.6 \pm 1.4 \pm 0.4^{+0.5}_{-0.9}$
6–7	$22.2 \pm 2.5 \pm 1.1^{+3.0}_{-5.6}$	$19.1 \pm 1.7 \pm 0.9^{+1.5}_{-3.0}$	$8.4 \pm 1.0 \pm 0.4^{+0.3}_{-0.6}$	$7.1 \pm 1.0 \pm 0.3^{+0.2}_{-0.3}$	$3.1 \pm 0.9 \pm 0.2^{+0.1}_{-0.3}$
7–8	$20.6 \pm 2.4 \pm 1.0^{+2.7}_{-5.4}$	$10.5 \pm 1.2 \pm 0.5^{+0.8}_{-1.6}$	$9.2 \pm 1.1 \pm 0.4^{+0.3}_{-0.6}$	$5.2 \pm 0.9 \pm 0.3^{+0.1}_{-0.1}$	$1.4 \pm 0.6 \pm 0.1^{+0.1}_{-0.1}$
8–9	$13.7 \pm 1.9 \pm 0.7^{+1.7}_{-3.3}$	$10.7 \pm 1.2 \pm 0.5^{+0.8}_{-1.6}$	$6.8 \pm 0.9 \pm 0.3^{+0.1}_{-0.3}$	$2.4 \pm 0.6 \pm 0.1^{+0.0}_{-0.1}$	$0.6 \pm 0.4 \pm 0.0^{+0.0}_{-0.0}$
9–10	$11.3 \pm 1.7 \pm 0.5^{+1.3}_{-2.5}$	$6.9 \pm 1.0 \pm 0.3^{+0.4}_{-0.8}$	$5.7 \pm 0.8 \pm 0.3^{+0.2}_{-0.3}$	$2.5 \pm 0.6 \pm 0.1^{+0.0}_{-0.1}$	$3.2 \pm 0.9 \pm 0.2^{+0.1}_{-0.1}$
10–11	$8.4 \pm 1.5 \pm 0.4^{+1.0}_{-2.0}$	$5.5 \pm 0.9 \pm 0.3^{+0.3}_{-0.6}$	$4.3 \pm 0.7 \pm 0.2^{+0.1}_{-0.2}$	$2.6 \pm 0.6 \pm 0.1^{+0.1}_{-0.1}$	–
11–12	$8.7 \pm 1.4 \pm 0.4^{+0.9}_{-1.7}$	$4.4 \pm 0.7 \pm 0.2^{+0.2}_{-0.3}$	$3.2 \pm 0.6 \pm 0.2^{+0.1}_{-0.2}$	$1.8 \pm 0.5 \pm 0.1^{+0.0}_{-0.1}$	–
12–13	$4.5 \pm 1.0 \pm 0.2^{+0.4}_{-0.9}$	$3.2 \pm 0.6 \pm 0.2^{+0.1}_{-0.3}$	$3.5 \pm 0.7 \pm 0.2^{+0.1}_{-0.1}$	–	–
13–14	$2.4 \pm 0.7 \pm 0.1^{+0.2}_{-0.4}$	$0.7 \pm 0.3 \pm 0.0^{+0.0}_{-0.1}$	$2.1 \pm 0.5 \pm 0.1^{+0.0}_{-0.1}$	–	–
14–15	$0.7 \pm 0.4 \pm 0.0^{+0.1}_{-0.1}$	$1.5 \pm 0.4 \pm 0.1^{+0.1}_{-0.1}$	$0.9 \pm 0.3 \pm 0.0^{+0.0}_{-0.0}$	–	–

is about a factor one hundred smaller than the integrated J/ψ cross-section in the identical region of p_T and y [26], and a factor three smaller than the integrated $\Upsilon(1S)$ cross-section in the central region, as measured by CMS [16] and ATLAS [15].

Figure 4 compares the LHCb measurement of the differential $\Upsilon(1S) \to \mu^+\mu^-$ production cross-section with several theory predictions in the LHCb acceptance region. In Fig. 4(a) the data are compared to direct production as calculated from a NNLO* colour-singlet model [29, 30], where the notation NNLO* denotes an evaluation that is not a complete next-to-next leading order computation and that can be affected by logarithmic corrections, which are not easily quantifiable. Direct production as calculated from NLO CSM is also represented. In Fig. 4(b) the data are compared to two model predictions for the $\Upsilon(1S)$ production: the calculation from NRQCD at NLO, including contributions from χ_b and higher Υ states decays, summing the colour-singlet and colour-octet contributions [31], and the calculation from the NLO CEM, including contributions from χ_b and higher Υ states decays [14]. Note that the NNLO* theoretical model computes the direct $\Upsilon(1S)$ production, whereas the LHCb measurement includes $\Upsilon(1S)$ from χ_b, $\Upsilon(2S)$ and $\Upsilon(3S)$ decays. However, taking into account the feed-down contribution, which has been measured to be of the order of 50 % [32], a satisfactory agreement is found with the theoretical predictions. Figure 5 compares the LHCb measurement of the differential $\Upsilon(2S)$ and $\Upsilon(3S)$ production cross-sections times branching fraction with the NNLO* theory predictions of direct production. It can be seen that the agreement with the theory is better for the $\Upsilon(3S)$, which is expected to be less affected by feed-down. At present there is no measurement of the contribution of feed-down to the $\Upsilon(2S)$ and $\Upsilon(3S)$ inclusive rate. The cross-sections times the dimuon branching fractions for the three Υ states are compared in Fig. 6 as a function of rapidity and transverse momentum. The cross-section results are used to evaluate the ratios $R^{iS/1S}$ of the $\Upsilon(2S)$ to $\Upsilon(1S)$ and $\Upsilon(3S)$ to $\Upsilon(1S)$ cross-sections times the dimuon branching fractions. Most of the systematic uncertainties on the cross-sections cancel in the ratio, except those due to the size of the data sample, the choice of fit function and the unknown polarisation of the different states. The polarisation uncertainty has been evaluated for the scenarios in which one of the two Υ states is completely polarised (either transversely or longitudinally) and the other is not polarised. The maximum difference of these two cases ranges between 15 % and 26 %. The ratios $R^{iS/1S}$, $i = 2, 3$, are given in Ta-
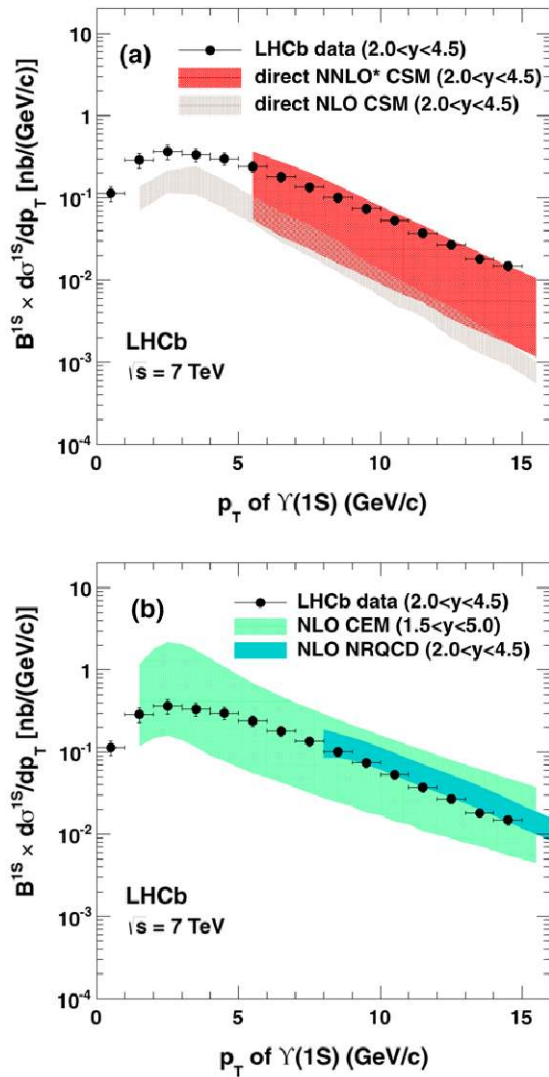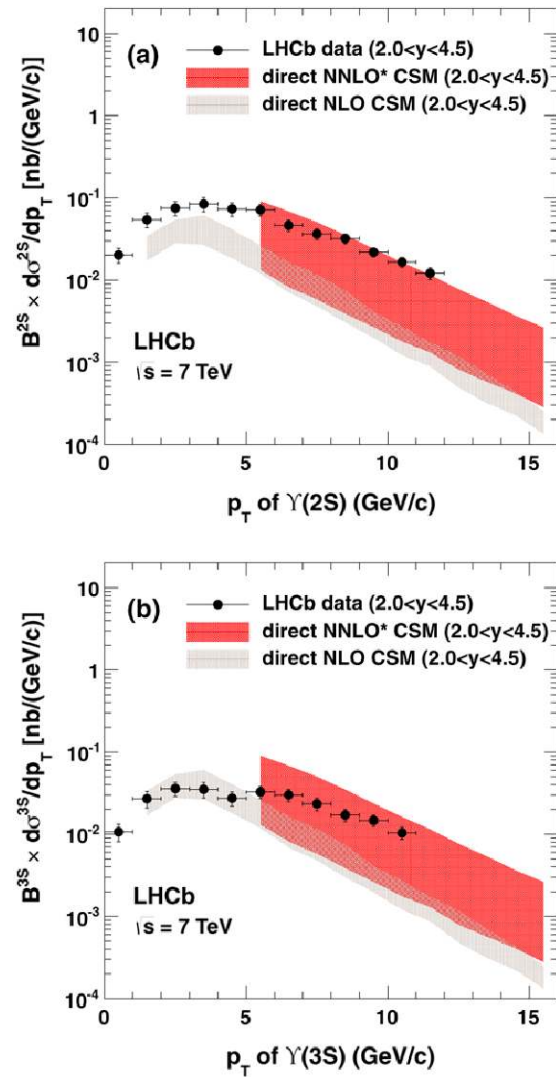
Fig. 4 Differential $\Upsilon(1S) \to \mu^+\mu^-$ production cross-section times dimuon branching fraction as a function of p_T integrated over y in the range 2.0–4.5, compared with the predictions from (**a**) the NNLO* CSM [29] for direct production, and (**b**) the NLO NRQCD [31] and CEM [14]. The *error bars* on the data correspond to the total uncertainties for each bin, while the bands indicate the uncertainty on the theory prediction

Fig. 5 Differential (**a**) $\Upsilon(2S) \to \mu^+\mu^-$ and (**b**) $\Upsilon(3S) \to \mu^+\mu^-$ production cross-sections times dimuon branching fractions as a function of p_T integrated over y in the range 2.0–4.5, compared with the predictions from the NNLO* CSM for direct production [29]. The *error bars* on the data correspond to the total uncertainties for each bin, while the bands indicate the uncertainty on the theory prediction

ble 5 and shown in Fig. 7. The polarisation uncertainty is not included in these figures. The results agree well with the corresponding ratio measurements from CMS [16] in the p_T range common to both experiments.

6 Conclusions

The differential cross-sections $\Upsilon(iS) \to \mu^+\mu^-$, for $i = 1, 2, 3$, are measured as a function of the Υ transverse momentum and rapidity in the region $p_T < 15$ GeV/c, $2.0 < y < 4.5$ in the LHCb experiment. The analysis is based on a data sample corresponding to an integrated luminosity of 25 pb^{-1} collected at the Large Hadron Collider at a centre-of-mass energy of $\sqrt{s} = 7$ TeV. The results obtained are compatible with previous measurements in pp collisions at the same centre-of-mass energy, performed by ATLAS and CMS in a different region of rapidity [15, 16]. This is the first measurement of Υ production in the forward region at $\sqrt{s} = 7$ TeV. A comparison with theoretical models shows good agreement with the measured Υ cross-sections. The measurement of the differential cross-sections is not sufficient to discriminate amongst the various models, and studies of other observables such as the Υ polarisations will be necessary.

Table 5 Ratios of cross-sections $\Upsilon(2S) \to \mu^+\mu^-$ and $\Upsilon(3S) \to \mu^+\mu^-$ with respect to $\Upsilon(1S) \to \mu^+\mu^-$ as a function of p_T in the range $2.0 < y < 4.5$, assuming no polarisation. The first uncertainty is statistical, the second is systematic and the third is due to the unknown polarisation of the three states

p_T (GeV/c)	$R^{2S/1S}$	$R^{3S/1S}$
0–1	$0.202 \pm 0.015 \pm 0.006 \pm 0.052$	$0.099 \pm 0.010 \pm 0.003 \pm 0.025$
1–2	$0.192 \pm 0.009 \pm 0.005 \pm 0.051$	$0.089 \pm 0.006 \pm 0.003 \pm 0.024$
2–3	$0.207 \pm 0.008 \pm 0.006 \pm 0.052$	$0.098 \pm 0.005 \pm 0.003 \pm 0.025$
3–4	$0.247 \pm 0.010 \pm 0.007 \pm 0.056$	$0.099 \pm 0.006 \pm 0.003 \pm 0.023$
4–5	$0.234 \pm 0.010 \pm 0.007 \pm 0.047$	$0.087 \pm 0.005 \pm 0.003 \pm 0.017$
5–6	$0.305 \pm 0.013 \pm 0.009 \pm 0.058$	$0.136 \pm 0.007 \pm 0.005 \pm 0.023$
6–7	$0.260 \pm 0.013 \pm 0.007 \pm 0.048$	$0.160 \pm 0.009 \pm 0.006 \pm 0.027$
7–8	$0.268 \pm 0.015 \pm 0.008 \pm 0.048$	$0.162 \pm 0.011 \pm 0.006 \pm 0.027$
8–9	$0.309 \pm 0.019 \pm 0.009 \pm 0.046$	$0.166 \pm 0.013 \pm 0.006 \pm 0.028$
9–10	$0.303 \pm 0.022 \pm 0.009 \pm 0.045$	$0.187 \pm 0.016 \pm 0.007 \pm 0.032$
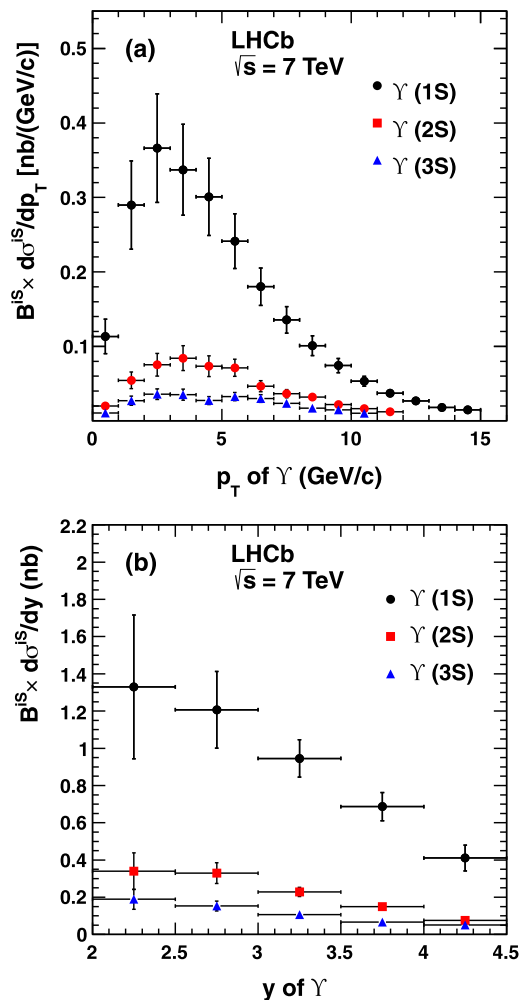
Fig. 6 Differential cross-sections of $\Upsilon(1S)$, $\Upsilon(2S)$ and $\Upsilon(3S)$ times dimuon branching fractions as a function of (**a**) p_T integrated over y and (**b**) y integrated over p_T. The *error bars* on the data correspond to the total uncertainties for each bin
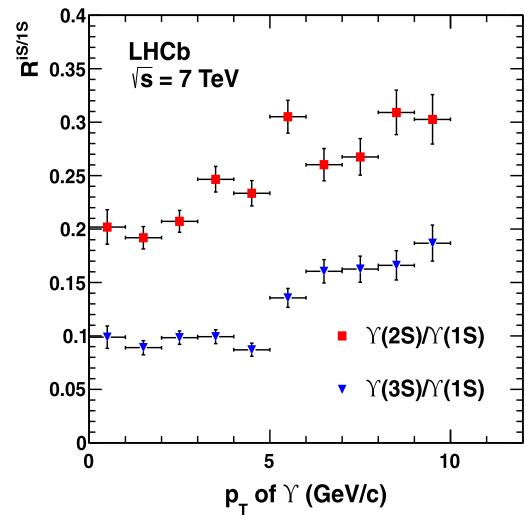
Fig. 7 Ratios of $\Upsilon(2S) \to \mu^+\mu^-$ and $\Upsilon(3S) \to \mu^+\mu^-$ with respect to $\Upsilon(1S) \to \mu^+\mu^-$ as a function of p_T of the Υ in the range $2.0 < y < 4.5$, assuming no polarisation. The *error bars* on the data correspond to the total uncertainties for each bin except for that due to the unknown polarisation, which ranges between 15 % and 26 % as listed in Table 5

References

1. A. Bondar et al. (Belle collaboration), Observation of two charged bottomonium-like resonances in $\Upsilon(5S)$ decays. arXiv:1110.2251
2. K.F. Chen et al. (Belle collaboration), Observation of anomalous $\Upsilon(1S)\pi^+\pi^-$ and $\Upsilon(2S)\pi^+\pi^-$ production near the $\Upsilon(5S)$ resonance. Phys. Rev. Lett. **100**, 112001 (2008). arXiv:0710.2577
3. I. Adachi et al. (Belle collaboration), First observation of the P-wave spin-singlet bottomonium states $h_b(1P)$ and $h_b(2P)$. Phys. Rev. Lett. **108**, 032001 (2012). arXiv:1103.3419
4. G. Aad et al. (ATLAS collaboration), Observation of a new χ_b state in radiative transitions to $\Upsilon(1S)$ and $\Upsilon(2S)$ at ATLAS. arXiv:1112.5154
5. D. Acosta et al. (CDF collaboration), Υ production and polarization in $p\bar{p}$ collisions at $\sqrt{s} = 1.8$ TeV. Phys. Rev. Lett. **88**, 161802 (2002)
6. V.M. Abazov et al. (D0 collaboration), Measurement of the polarization of the $\Upsilon(1S)$ and $\Upsilon(2S)$ states in $p\bar{p}$ collisions at $\sqrt{s} = 1.96$ TeV. Phys. Rev. Lett. **101**, 182004 (2008). arXiv:0804.2799
7. V.M. Abazov et al. (D0 collaboration), Measurement of inclusive differential cross sections for $\Upsilon(1S)$ production in $p\bar{p}$ collisions at $\sqrt{s} = 1.96$ TeV. Phys. Rev. Lett. **94**, 232001 (2005). arXiv:hep-ex/0502030
8. C.-H. Chang, Hadronic production of J/ψ associated with a gluon. Nucl. Phys. B **172**, 425 (1980)
9. R. Baier, R. Rückl, Hadronic collisions: a quarkonium factory. Z. Phys. C **19**, 251 (1983)
10. R. Baier, R. Rückl, Hadronic production of J/ψ and Υ: transverse momentum distributions. Phys. Lett. B **102**, 364 (1981)
11. G.T. Bodwin, E. Braaten, G.P. Lepage, Rigorous QCD analysis of inclusive annihilation and production of heavy quarkonium. Phys. Rev. D **51**, 1125 (1995). arXiv:hep-ph/9407339
12. P. Cho, A.K. Leibovich, Color-octet quarkonia production. Phys. Rev. D **53**, 150 (1996). arXiv:hep-ph/9505329
13. P. Cho, A.K. Leibovich, Color-octet quarkonia production II. Phys. Rev. D **53**, 6203 (1996). arXiv:hep-ph/9511315
14. A.D. Frawley, T. Ullrich, R. Vogt, Heavy flavor in heavy-ion collisions at RHIC and RHIC II. Phys. Rep. **462**, 125 (2008). arXiv:0806.1013
15. G. Aad et al. (ATLAS collaboration), Measurement of the $\Upsilon(1S)$ production cross-section in pp collisions at $\sqrt{s} = 7$ TeV in ATLAS. Phys. Lett. B **705**, 9 (2011). arXiv:1106.5325
16. V. Khachatryan et al. (CMS collaboration), Measurement of the inclusive Υ production cross section in pp collisions at $\sqrt{s} = 7$ TeV. Phys. Rev. D **83**, 112004 (2011). arXiv:1012.5545
17. A.A. Alves Jr. et al. (LHCb collaboration), The LHCb detector at the LHC. J. Instrum. **3**, S08005 (2008)
18. T. Sjöstrand, S. Mrenna, P. Skands, PYTHIA 6.4 physics and manual. J. High Energy Phys. **05**, 026 (2006). arXiv:hep-ph/0603175
19. I. Belyaev et al., Handling of the generation of primary events in GAUSS, the LHCb simulation framework, in *Nuclear Science Symposium Conference Record (NSS/MIC)* (IEEE, ???, 2010), p. 1155
20. D.J. Lange, The EvtGen particle decay simulation package. Nucl. Instrum. Methods A **462**, 152 (2001)
21. S. Agostinelli et al. (GEANT4 collaboration), GEANT4: a simulation toolkit. Nucl. Instrum. Methods A **506**, 250 (2003)
22. P. Golonka, Z. Was, PHOTOS Monte Carlo: a precision tool for QED corrections in Z and W decays. Eur. Phys. J. C **45**, 97 (2006). arXiv:hep-ph/0506026
23. T. Skwarnicki, A study of the radiative cascade transitions between the Upsilon-prime and Upsilon resonances. PhD thesis, Institute of Nuclear Physics, Krakow, 1986. DESY-F31-86-02
24. M. Ferro-Luzzi, Proposal for an absolute luminosity determination in colliding beam experiments using vertex detection of beam–gas interactions. Nucl. Instrum. Methods A **553**, 388 (2005)
25. R. Aaij et al. (LHCb collaboration), Absolute luminosity measurements with the LHCb detector at the LHC. J. Instrum. **7**, P01010 (2012). arXiv:1110.2866
26. R. Aaij et al. (LHCb collaboration), Measurement of J/ψ production in pp collisions at $\sqrt{s} = 7$ TeV. Eur. Phys. J. C **71**, 1645 (2011). arXiv:1103.0423
27. C.S. Lam, W.-K. Tung, A systematic approach to inclusive lepton pair production in hadronic collisions. Phys. Rev. D **18**, 2447 (1978)
28. M. De Cian et al., Tracking performance of the LHCb spectrometer. LHCb-PROC-2011-057
29. P. Artoisenet, J.M. Campbell, J.P. Lansberg, F. Maltoni, F. Tramontano, Upsilon production at fermilab tevatron and LHC energies. Phys. Rev. Lett. **101**, 152001 (2008). arXiv:0806.3282
30. J.M. Campbell, F. Maltoni, F. Tramontano, QCD corrections to J/ψ and Upsilon production at hadron colliders. Phys. Rev. Lett. **98**, 252002 (2007). arXiv:hep-ph/0703113
31. Y.-Q. Ma, K. Wang, K.-T. Chao, J/ψ (ψ') production at the Tevatron and LHC at $O(\alpha_s^4 v^4)$ in nonrelativistic QCD. Phys. Rev. Lett. **106**, 042002 (2011). arXiv:1009.3655
32. T. Affolder et al. (CDF collaboration), Production of $\Upsilon(1S)$ mesons from χ_b decays in $p\bar{p}$ collisions at $\sqrt{s} = 1.8$ TeV. Phys. Rev. Lett. **84**, 2094 (2000). arXiv:hep-ex/9910025

The LHCb Collaboration

R. Aaij[38], C. Abellan Beteta[33,n], B. Adeva[34], M. Adinolfi[43], C. Adrover[6], A. Affolder[49], Z. Ajaltouni[5], J. Albrecht[35], F. Alessio[35], M. Alexander[48], G. Alkhazov[27], P. Alvarez Cartelle[34], A.A. Alves Jr[22], S. Amato[2], Y. Amhis[36], J. Anderson[37], R.B. Appleby[51], O. Aquines Gutierrez[10], F. Archilli[18,35], L. Arrabito[55,q], A. Artamonov[32], M. Artuso[53,35], E. Aslanides[6], G. Auriemma[22,m], S. Bachmann[11], J.J. Back[45], D.S. Bailey[51], V. Balagura[28,35], W. Baldini[16], R.J. Barlow[51], C. Barschel[35], S. Barsuk[7], W. Barter[44], A. Bates[48], C. Bauer[10], Th. Bauer[38], A. Bay[36], I. Bediaga[1], S. Belogurov[28], K. Belous[32], I. Belyaev[28], E. Ben-Haim[8], M. Benayoun[8], G. Bencivenni[18], S. Benson[47], J. Benton[43], R. Bernet[37], M.-O. Bettler[17], M. van Beuzekom[38], A. Bien[11], S. Bifani[12], T. Bird[51], A. Bizzeti[17,h], P.M. Bjørnstad[51], T. Blake[35],

F. Blanc[36], C. Blanks[50], J. Blouw[11], S. Blusk[53], A. Bobrov[31], V. Bocci[22], A. Bondar[31], N. Bondar[27], W. Bonivento[15], S. Borghi[48,51], A. Borgia[53], T.J.V. Bowcock[49], C. Bozzi[16], T. Brambach[9], J. van den Brand[39], J. Bressieux[36], D. Brett[51], M. Britsch[10], T. Britton[53], N.H. Brook[43], H. Brown[49], K. de Bruyn[38], A. Büchler-Germann[37], I. Burducea[26], A. Bursche[37], J. Buytaert[35], S. Cadeddu[15], O. Callot[7], M. Calvi[20,j], M. Calvo Gomez[33,n], A. Camboni[33], P. Campana[18,35], A. Carbone[14], G. Carboni[21,k], R. Cardinale[19,35,i], A. Cardini[15], L. Carson[50], K. Carvalho Akiba[2], G. Casse[49], M. Cattaneo[35], Ch. Cauet[9], M. Charles[52], Ph. Charpentier[35], N. Chiapolini[37], K. Ciba[35], X. Cid Vidal[34], G. Ciezarek[50], P.E.L. Clarke[47,35], M. Clemencic[35], H.V. Cliff[44], J. Closier[35], C. Coca[26], V. Coco[38], J. Cogan[6], P. Collins[35], A. Comerma-Montells[33], F. Constantin[26], A. Contu[52], A. Cook[43], M. Coombes[43], G. Corti[35], B. Couturier[35], G.A. Cowan[36], R. Currie[47], C. D'Ambrosio[35], P. David[8], P.N.Y. David[38], I. De Bonis[4], S. De Capua[21,k], M. De Cian[37], F. De Lorenzi[12], J.M. De Miranda[1], L. De Paula[2], P. De Simone[18], D. Decamp[4], M. Deckenhoff[9], H. Degaudenzi[36,35], L. Del Buono[8], C. Deplano[15], D. Derkach[14,35], O. Deschamps[5], F. Dettori[39], J. Dickens[44], H. Dijkstra[35], P. Diniz Batista[1], F. Domingo Bonal[33,n], S. Donleavy[49], F. Dordei[11], A. Dosil Suárez[34], D. Dossett[45], A. Dovbnya[40], F. Dupertuis[36], R. Dzhelyadin[32], A. Dziurda[23], S. Easo[46], U. Egede[50], V. Egorychev[28], S. Eidelman[31], D. van Eijk[38], F. Eisele[11], S. Eisenhardt[47], R. Ekelhof[9], L. Eklund[48], Ch. Elsasser[37], D. Elsby[42], D. Esperante Pereira[34], A. Falabella[16,14,e], E. Fanchini[20,j], C. Färber[11], G. Fardell[47], C. Farinelli[38], S. Farry[12], V. Fave[36], V. Fernandez Albor[34], M. Ferro-Luzzi[35], S. Filippov[30], C. Fitzpatrick[47], M. Fontana[10], F. Fontanelli[19,i], R. Forty[35], O. Francisco[2], M. Frank[35], C. Frei[35], M. Frosini[17,f], S. Furcas[20], A. Gallas Torreira[34], D. Galli[14,c], M. Gandelman[2], P. Gandini[52], Y. Gao[3], J-C. Garnier[35], J. Garofoli[53], J. Garra Tico[44], L. Garrido[33], D. Gascon[33], C. Gaspar[35], R. Gauld[52], N. Gauvin[36], M. Gersabeck[35], T. Gershon[45,35], Ph. Ghez[4], V. Gibson[44], V.V. Gligorov[35], C. Göbel[54,p], D. Golubkov[28], A. Golutvin[50,28,35], A. Gomes[2], H. Gordon[52], M. Grabalosa Gándara[33], R. Graciani Diaz[33], L.A. Granado Cardoso[35], E. Graugés[33], G. Graziani[17], A. Grecu[26], E. Greening[52], S. Gregson[44], B. Gui[53], E. Gushchin[30], Yu. Guz[32], T. Gys[35], C. Hadjivasiliou[53], G. Haefeli[36], C. Haen[35], S.C. Haines[44], T. Hampson[43], S. Hansmann-Menzemer[11], R. Harji[50], N. Harnew[52], J. Harrison[51], P.F. Harrison[45], T. Hartmann[56,r], J. He[7], V. Heijne[38], K. Hennessy[49], P. Henrard[5], J.A. Hernando Morata[34], E. van Herwijnen[35], E. Hicks[49], K. Holubyev[11], P. Hopchev[4], W. Hulsbergen[38], P. Hunt[52], T. Huse[49], R.S. Huston[12], D. Hutchcroft[49], D. Hynds[48], V. Iakovenko[41], P. Ilten[12], J. Imong[43], R. Jacobsson[35], A. Jaeger[11], M. Jahjah Hussein[5], E. Jans[38], F. Jansen[38], P. Jaton[36], B. Jean-Marie[7], F. Jing[3], M. John[52], D. Johnson[52], C.R. Jones[44], B. Jost[35], M. Kaballo[9], S. Kandybei[40], M. Karacson[35], T.M. Karbach[9], J. Keaveney[12], I.R. Kenyon[42], U. Kerzel[35], T. Ketel[39], A. Keune[36], B. Khanji[6], Y.M. Kim[47], M. Knecht[36], R.F. Koopman[39], P. Koppenburg[38], M. Korolev[29], A. Kozlinskiy[38], L. Kravchuk[30], K. Kreplin[11], M. Kreps[45], G. Krocker[11], P. Krokovny[11], F. Kruse[9], K. Kruzelecki[35], M. Kucharczyk[20,23,35,j], T. Kvaratskheliya[28,35], V.N. La Thi[36], D. Lacarrere[35], G. Lafferty[51], A. Lai[15], D. Lambert[47], R.W. Lambert[39], E. Lanciotti[35], G. Lanfranchi[18], C. Langenbruch[11], T. Latham[45], C. Lazzeroni[42], R. Le Gac[6], J. van Leerdam[38], J.-P. Lees[4], R. Lefèvre[5], A. Leflat[29,35], J. Lefrançois[7], O. Leroy[6], T. Lesiak[23], L. Li[3], L. Li Gioi[5], M. Lieng[9], M. Liles[49], R. Lindner[35], C. Linn[11], B. Liu[3], G. Liu[35], J. von Loeben[20], J.H. Lopes[2], E. Lopez Asamar[33], N. Lopez-March[36], H. Lu[3], J. Luisier[36], A. Mac Raighne[48], F. Machefert[7], I.V. Machikhiliyan[4,28], F. Maciuc[10], O. Maev[27,35], J. Magnin[1], S. Malde[52], R.M.D. Mamunur[35], G. Manca[15,d], G. Mancinelli[6], N. Mangiafave[44], U. Marconi[14], R. Märki[36], J. Marks[11], G. Martellotti[22], A. Martens[8], L. Martin[52], A. Martín Sánchez[7], D. Martinez Santos[35], A. Massafferri[1], Z. Mathe[12], C. Matteuzzi[20], M. Matveev[27], E. Maurice[6], B. Maynard[53], A. Mazurov[16,30,35], G. McGregor[51], R. McNulty[12], M. Meissner[11], M. Merk[38], J. Merkel[9], R. Messi[21,k], S. Miglioranzi[35], D.A. Milanes[13], M.-N. Minard[4], J. Molina Rodriguez[54,p], S. Monteil[5], D. Moran[12], P. Morawski[23], R. Mountain[53], I. Mous[38], F. Muheim[47], K. Müller[37], R. Muresan[26], B. Muryn[24], B. Muster[36], M. Musy[33], J. Mylroie-Smith[49], P. Naik[43], T. Nakada[36], R. Nandakumar[46], I. Nasteva[1], M. Nedos[9], M. Needham[47], N. Neufeld[35], A.D. Nguyen[36], C. Nguyen-Mau[36,o], M. Nicol[7], V. Niess[5], N. Nikitin[29], A. Nomerotski[52,35], A. Novoselov[32], A. Oblakowska-Mucha[24], V. Obraztsov[32], S. Oggero[38], S. Ogilvy[48], O. Okhrimenko[41], R. Oldeman[15,35,d], M. Orlandea[26], J.M. Otalora Goicochea[2], P. Owen[50], K. Pal[53], J. Palacios[37], A. Palano[13,b], M. Palutan[18], J. Panman[35], A. Papanestis[46], M. Pappagallo[48], C. Parkes[51], C.J. Parkinson[50], G. Passaleva[17], G.D. Patel[49], M. Patel[50], S.K. Paterson[50], G.N. Patrick[46], C. Patrignani[19,i], C. Pavel-Nicorescu[26], A. Pazos Alvarez[34], A. Pellegrino[38], G. Penso[22,l], M. Pepe Altarelli[35], S. Perazzini[14,c], D.L. Perego[20,j], E. Perez Trigo[34], A. Pérez-Calero Yzquierdo[33], P. Perret[5], M. Perrin-Terrin[6], G. Pessina[20], A. Petrella[16,35], A. Petrolini[19,i], A. Phan[53], E. Picatoste Olloqui[33], B. Pie Valls[33], B. Pietrzyk[4], T. Pilař[45], D. Pinci[22], R. Plackett[48], S. Playfer[47], M. Plo Casasus[34], G. Polok[23], A. Poluektov[45,31], E. Polycarpo[2], D. Popov[10], B. Popovici[26], C. Potterat[33], A. Powell[52], J. Prisciandaro[36], V. Pugatch[41], A. Puig Navarro[33], W. Qian[53], J.H. Rademacker[43], B. Rakotomiaramanana[36], M.S. Rangel[2], I. Raniuk[40], G. Raven[39], S. Redford[52], M.M. Reid[45], A.C. dos Reis[1], S. Ricciardi[46], A. Richards[50], K. Rinnert[49], D.A. Roa Romero[5], P. Robbe[7], E. Rodrigues[48,51], F. Rodrigues[2], P. Rodriguez Perez[34], G.J. Rogers[44], S. Roiser[35], V. Romanovsky[32], M. Rosello[33,n], J. Rouvinet[36], T. Ruf[35], H. Ruiz[33], G. Sabatino[21,k], J.J. Saborido Silva[34], N. Sagidova[27], P. Sail[48], B. Saitta[15,d], C. Salzmann[37], M. Sannino[19,i], R. Santacesaria[22], C. Santamarina Rios[34], R. Santinelli[35], E. Santovetti[21,k], M. Sapunov[6], A. Sarti[18,l], C. Satriano[22,m], A. Satta[21], M. Savrie[16,e], D. Savrina[28], P. Schaack[50], M. Schiller[39],

S. Schleich[9], M. Schlupp[9], M. Schmelling[10], B. Schmidt[35], O. Schneider[36], A. Schopper[35], M.-H. Schune[7], R. Schwemmer[35], B. Sciascia[18], A. Sciubba[18,l], M. Seco[34], A. Semennikov[28], K. Senderowska[24], I. Sepp[50], N. Serra[37], J. Serrano[6], P. Seyfert[11], M. Shapkin[32], I. Shapoval[40,35], P. Shatalov[28], Y. Shcheglov[27], T. Shears[49], L. Shekhtman[31], O. Shevchenko[40], V. Shevchenko[28], A. Shires[50], R. Silva Coutinho[45], T. Skwarnicki[53], N.A. Smith[49], E. Smith[52,46], K. Sobczak[5], F.J.P. Soler[48], A. Solomin[43], F. Soomro[18,35], B. Souza De Paula[2], B. Spaan[9], A. Sparkes[47], P. Spradlin[48], F. Stagni[35], S. Stahl[11], O. Steinkamp[37], S. Stoica[26], S. Stone[53,35], B. Storaci[38], M. Straticiuc[26], U. Straumann[37], V.K. Subbiah[35], S. Swientek[9], M. Szczekowski[25], P. Szczypka[36], T. Szumlak[24], S. T'Jampens[4], E. Teodorescu[26], F. Teubert[35], C. Thomas[52], E. Thomas[35], J. van Tilburg[11], V. Tisserand[4], M. Tobin[37], S. Topp-Joergensen[52], N. Torr[52], E. Tournefier[4,50], S. Tourneur[36], M.T. Tran[36], A. Tsaregorodtsev[6], N. Tuning[38], M. Ubeda Garcia[35], A. Ukleja[25], P. Urquijo[53], U. Uwer[11], V. Vagnoni[14], G. Valenti[14], R. Vazquez Gomez[33], P. Vazquez Regueiro[34], S. Vecchi[16], J.J. Velthuis[43], M. Veltri[17,g], B. Viaud[7], I. Videau[7], D. Vieira[2], X. Vilasis-Cardona[33,n], J. Visniakov[34], A. Vollhardt[37], D. Volyanskyy[10], D. Voong[43], A. Vorobyev[27], H. Voss[10], S. Wandernoth[11], J. Wang[53], D.R. Ward[44], N.K. Watson[42], A.D. Webber[51], D. Websdale[50], M. Whitehead[45], D. Wiedner[11], L. Wiggers[38], G. Wilkinson[52], M.P. Williams[45,46], M. Williams[50], F.F. Wilson[46], J. Wishahi[9], M. Witek[23], W. Witzeling[35], S.A. Wotton[44], K. Wyllie[35], Y. Xie[47], F. Xing[52], Z. Xing[53], Z. Yang[3], R. Young[47], O. Yushchenko[32], M. Zangoli[14], M. Zavertyaev[10,a], F. Zhang[3], L. Zhang[53], W.C. Zhang[12], Y. Zhang[3], A. Zhelezov[11], L. Zhong[3], A. Zvyagin[35]

[1]Centro Brasileiro de Pesquisas Físicas (CBPF), Rio de Janeiro, Brazil

[2]Universidade Federal do Rio de Janeiro (UFRJ), Rio de Janeiro, Brazil

[3]Center for High Energy Physics, Tsinghua University, Beijing, China

[4]LAPP, Université de Savoie, CNRS/IN2P3, Annecy-Le-Vieux, France

[5]Clermont Université, Université Blaise Pascal, CNRS/IN2P3, LPC, Clermont-Ferrand, France

[6]CPPM, Aix-Marseille Université, CNRS/IN2P3, Marseille, France

[7]LAL, Université Paris-Sud, CNRS/IN2P3, Orsay, France

[8]LPNHE, Université Pierre et Marie Curie, Université Paris Diderot, CNRS/IN2P3, Paris, France

[9]Fakultät Physik, Technische Universität Dortmund, Dortmund, Germany

[10]Max-Planck-Institut für Kernphysik (MPIK), Heidelberg, Germany

[11]Physikalisches Institut, Ruprecht-Karls-Universität Heidelberg, Heidelberg, Germany

[12]School of Physics, University College Dublin, Dublin, Ireland

[13]Sezione INFN di Bari, Bari, Italy

[14]Sezione INFN di Bologna, Bologna, Italy

[15]Sezione INFN di Cagliari, Cagliari, Italy

[16]Sezione INFN di Ferrara, Ferrara, Italy

[17]Sezione INFN di Firenze, Firenze, Italy

[18]Laboratori Nazionali dell'INFN di Frascati, Frascati, Italy

[19]Sezione INFN di Genova, Genova, Italy

[20]Sezione INFN di Milano Bicocca, Milano, Italy

[21]Sezione INFN di Roma Tor Vergata, Roma, Italy

[22]Sezione INFN di Roma La Sapienza, Roma, Italy

[23]Henryk Niewodniczanski Institute of Nuclear Physics Polish Academy of Sciences, Kraków, Poland

[24]AGH University of Science and Technology, Kraków, Poland

[25]Soltan Institute for Nuclear Studies, Warsaw, Poland

[26]Horia Hulubei National Institute of Physics and Nuclear Engineering, Bucharest-Magurele, Romania

[27]Petersburg Nuclear Physics Institute (PNPI), Gatchina, Russia

[28]Institute of Theoretical and Experimental Physics (ITEP), Moscow, Russia

[29]Institute of Nuclear Physics, Moscow State University (SINP MSU), Moscow, Russia

[30]Institute for Nuclear Research of the Russian Academy of Sciences (INR RAN), Moscow, Russia

[31]Budker Institute of Nuclear Physics (SB RAS) and Novosibirsk State University, Novosibirsk, Russia

[32]Institute for High Energy Physics (IHEP), Protvino, Russia

[33]Universitat de Barcelona, Barcelona, Spain

[34]Universidad de Santiago de Compostela, Santiago de Compostela, Spain

[35]European Organization for Nuclear Research (CERN), Geneva, Switzerland

[36]Ecole Polytechnique Fédérale de Lausanne (EPFL), Lausanne, Switzerland

[37]Physik-Institut, Universität Zürich, Zürich, Switzerland

[38]Nikhef National Institute for Subatomic Physics, Amsterdam, The Netherlands

[39]Nikhef National Institute for Subatomic Physics and Vrije Universiteit, Amsterdam, The Netherlands

[40]NSC Kharkiv Institute of Physics and Technology (NSC KIPT), Kharkiv, Ukraine

[41]Institute for Nuclear Research of the National Academy of Sciences (KINR), Kyiv, Ukraine

[42]University of Birmingham, Birmingham, United Kingdom

[43]H.H. Wills Physics Laboratory, University of Bristol, Bristol, United Kingdom

[44]Cavendish Laboratory, University of Cambridge, Cambridge, United Kingdom

[45]Department of Physics, University of Warwick, Coventry, United Kingdom

[46]STFC Rutherford Appleton Laboratory, Didcot, United Kingdom

[47]School of Physics and Astronomy, University of Edinburgh, Edinburgh, United Kingdom

[48]School of Physics and Astronomy, University of Glasgow, Glasgow, United Kingdom

[49]Oliver Lodge Laboratory, University of Liverpool, Liverpool, United Kingdom

[50]Imperial College London, London, United Kingdom

[51]School of Physics and Astronomy, University of Manchester, Manchester, United Kingdom

[52]Department of Physics, University of Oxford, Oxford, United Kingdom

[53]Syracuse University, Syracuse, NY, United States

[54]Pontifícia Universidade Católica do Rio de Janeiro (PUC-Rio), Rio de Janeiro, Brazil

[55]CC-IN2P3, CNRS/IN2P3, Lyon-Villeurbanne, France

[56]Physikalisches Institut, Universität Rostock, Rostock, Germany

[a]P.N. Lebedev Physical Institute, Russian Academy of Science (LPI RAS), Moscow, Russia

[b]Università di Bari, Bari, Italy

[c]Università di Bologna, Bologna, Italy

[d]Università di Cagliari, Cagliari, Italy

[e]Università di Ferrara, Ferrara, Italy

[f]Università di Firenze, Firenze, Italy

[g]Università di Urbino, Urbino, Italy

[h]Università di Modena e Reggio Emilia, Modena, Italy

[i]Università di Genova, Genova, Italy

[j]Università di Milano Bicocca, Milano, Italy

[k]Università di Roma Tor Vergata, Roma, Italy

[l]Università di Roma La Sapienza, Roma, Italy

[m]Università della Basilicata, Potenza, Italy

[n]LIFAELS, La Salle, Universitat Ramon Llull, Barcelona, Spain

[o]Hanoi University of Science, Hanoi, Viet Nam

[p]Associated to Universidade Federal do Rio de Janeiro (UFRJ), Rio de Janeiro, Brazil

[q]Associated member

[r]Associated to Physikalisches Institut, Ruprecht-Karls-Universität Heidelberg, Heidelberg, Germany